Journal of Solid State Chemistry **159,** 1–6 (2001)
doi:10.1006/jssc.2001.9112, available online at http://www.idealibrary.com on IDEAL®

Temperature Dependence of the Hyperfine Interaction at ^{181}Ta in SrHfO$_3$

Alberto López-Garcia,[1] Patricia de la Presa,[2] and Alejandro Ayala[3]

Programa TENAES, Departamento de Física, Universidad Nacional de La Plata, C.C.67, 1900 La Plata, Argentina

Received November 1, 2000; accepted January 19, 2001; published online May 11, 2001

The temperature dependence of the quadrupole hyperfine parameters covering the temperature range from 293 to 1173 K has been measured at ^{181}Ta probes in SrHfO$_3$ by perturbed angular correlation spectroscopy. A fluctuating distribution of quadrupole interactions model has been applied to interpret the data. At low temperatures above $\sim$300 K a static, asymmetric, and distributed electric quadrupole interaction was detected. At intermediate temperatures ($\approx$600 K) a different quadrupole interaction appears, characterized by a fluctuating distribution of axially symmetric electric field gradient tensors. Above 873 K, the unique presence of a nuclear spin relaxation machanism shows a second change in the perturbation acting on probes. These changes in the hyperfine interaction are consistent with the structural phase transitions detected by diffraction techniques. The probe effects were also analyzed, comparing ^{181}Ta with ^{111}Cd experiments. © 2001 Academic Press

INTRODUCTION

The AMO_3 compounds display complex structural instabilities and electronic properties determined by A and M cations. Owing to their varied structure these materials have attracted interest in many applied and fundamental areas of advanced materials and solid-state research. These oxides usually have cubic, tetragonal, or orthorhombic structures. Anions surrounding M atoms form regular octahedra in crystals with cubic symmetry or distorted octahedra in crystals with lower symmetries. The A cations complete the structure, sitting at the vertices of the body.

Of the many compounds that can be formed, we are particularly interested in the ones in which A is an alkaline earth (Ca, Sr, or Ba) and M is Hf (a tetravalent metal). At room temperature (RT) CaHfO$_3$ and BaHfO$_3$ have orthorhombic and cubic structures, respectively.

Strontium hafnate has been a well known compound for a long time, but there has been no agreement about its crystalline structure. Through X-ray diffraction experiments Hoffman (1) determined a cubic structure with $a = 4.077$ Å; meanwhile Náray-Szabó (2) and Red'ko *et al.* (3) described it as orthorhombic and Jona and Shirane (4) reported it as having a cubic or pseudocubic lattice. Recently Guevara and coworkers using powder X-ray diffraction refined the structure of SrHfO$_3$ at different temperatures (5). At room temperature they found an orthorhombic (*Pnma*) structure that transforms into orthorhombic (*Imma*) at about 650 K and into cubic (*Pm*3*m*) above 950 K. Using powder neutron diffraction analysis, Kennedy *et al.* reproduced the RT result of Ref. (5) but proposed different high-temperature structures: orthorhombic (*Pnma* for $\text{RT} \leq T \leq 673$ K), orthorhombic (*Cmcm* at $T = 873$ K), tetragonal (*I*4/*mcm* for $1023 \leq T \leq 1353$ K), and cubic (*Pm*3*m* for $T > 1353$ K) (6). Using group theoretical analysis Howard and Stokes found that the *Pm*3*m* → *I*4/*mcm* → *Cmcm* transitions could be continuous and there would not be a continuous path in the *Cmcm* → *Pnma* transition.

The unusual characteristics of these compounds are mainly determined by the electron distribution associated with the oxygen-4$^+$–metal covalent bond. One way to study this electron distribution is by means of the hyperfine interactions. These compounds being non-nonmagnetic perovskites, their electron density is manifested through the components of the electric field gradient (EFG) tensor measured at the M site. Detailed electronic structure calculations (7, 8) show that the EFG measured at this site is predominantly originated by O-2p and M-nd hybridization.

Perturbed angular correlation spectroscopy (PAC) measures the nuclear spin precession produced by an extranuclear field. From this spin precession the EFG can be determined if a suitable probe is localized at the M site. PAC measurements were performed in CaHfO$_3$ (9), BaHfO$_3$ (10, 11), SrHfO$_3$ (12), and BaHfO$_3$ using ^{181}Ta and ^{111}Cd probes, respectively.

The hyperfine interaction at RT detected by ^{181}Ta probes in CaHfO$_3$ and BaHfO$_3$ is characterized by the quadrupole parameters $V_{zz} = 4.2_2 \times 10^{17}$ V/cm^2, $\eta = 0.67_2$, $\delta = 0.05_1$, and $\lambda = 45_3$ MHz, respectively. Andrade *et al.* (13) studied

---

[1] Member of Carrera de Investigador Científico, CONICET, Argentina.
[2] Fellowship of DAAD, Germany.
[3] Fellowship of CNPq, Brasil.

0022-4596/01 $35.00

$SrHfO_3$ and, for the strongest component of the EFG tensor, determined the quantity $V_{zz} = 2.3 \times 10^{17}$ V/cm^2. The complete set of hyperfine parameters were not reported by these authors and in their spectrum there seems to be a significant amount of HfO_2, which could hinder the determination of the asymmetry parameter (η) and the line width (δ).

The study of the quadrupole interaction at ^{111}Cd probe in $SrHfO_3$ showed that a fluctuating distribution of quadrupole interaction model had to be fitted to the measured time spectra. The hyperfine parameters determined at RT (12) were $V_{zz} = 1.2_1 \times 10^{17}$ V/cm^2, $\eta = 0.51_6$, $\delta = 0.13_1$, and $\lambda = 2.1_4$ MHz.

The aim of this work is twofold: (a) to measure by PAC the temperature dependence of the EFG at ^{181}Ta in $SrHfO_3$ and (b) to determine probe effects related to the coupling of impurity states to the lattice and how the structural phase transitions is manifested through the hyperfine parameters.

EXPERIMENT

The sample was prepared by the standard ceramic technique, using stoichiometric amounts of $SrCO_3$ and HfO_2. The powder was mixed, ground, and fired several times at 1273 K for a total time of 96 h. Then part of the as-prepared sample was analyzed by X-ray diffraction. Using the Rietveld procedure the reported lattice parameters were reproduced (5, 6). The other part was capsulated and sealed in a quartz tube for thermal neutron irradiation to produce ^{181}Hf. The sample was irradiated in a flux of 1.6×10^{13} particles cm^{-2} s^{-1} for 2 h at approximately 330 K.

The "as-irradiated" sample was PAC analyzed using a two-CsF-detector spectrometer with a time resolution of 0.7 ns for the 137- to 482-keV gamma–gamma cascade of ^{181}Ta. The sample was heat-treated *in situ* in a furnace with a thermal stability of 1 K. Coincidences were repeatedly accumulated during 15 min at 90°, 180°, and 270°. Each run took 24 h. The time spectra were obtained from RT to 1173 K, with temperature steps of 100 K. After the measurement at 1173 K and a sample annealing *in situ* at $\sim$900 K for 3 days a final measurement at RT was done.

The spin precession curves $R(t)$ were calculated from the time coincidence spectra. A nonlinear fit procedure was used to adjust the function,

$$R(t) = A_{22} \sum_i f_i G^i_{22}(t) + c_0, \qquad [1]$$

to the data. A_{22} is the anisotropy of the gamma–gamma cascade, f_i is the fraction of probes at ith site, and $G^i_{22}(t)$ is its perturbation factor, given by

$$G_{22}(t) = e^{-\lambda_2 t} \sum_n \sigma_{2n} \cos(\omega_n t) e^{-(\delta\omega_n t)^2/2}, \qquad [2]$$

where the ω_ns depend on ω_Q and η (with $\omega_Q = (eQV_{zz})/4I(2I-1)\hbar$ and $\eta = [V_{xx} - V_{yy}]/V_{zz}$), σ_ns are functions of η, and δ is the Gaussian distribution relative width or line broadening to describe lattice distortions. The λ_2 parameter is related to dynamic effects and c_0 is a constant baseline that could represent either probes in cubic sites or systematic errors in the measurements or the data analysis. This model has been successfully applied (13) to the analysis of the time spectra of ^{111}Cd in $SrHfO_3$.

The effects of time-dependent fields have been studied so far. The perturbation of angular correlation produced by rapid and isotropic fluctuations, as they occur in liquids, can be successfully described by the Abragam and Pound first-order perturbation theory. The stochastic models of Blume (14) and Winkler and Gerdau (15) are appropriate for more general cases of discrete jumps that may involve strong changes in the interaction. The very time-consuming procedure for precisely computing Blume's formalism has stimulated efforts to find approximate forms of the perturbation function $G_{kk}(t)$.

Baudry and Boyer (16) and Forker *et al.* (17) have shown that Eq. [2] can be used to describe dynamic perturbations for two opposite time rates. For fast fluctuations $\lambda_2 = 100.8\,(\omega_{Q,f})^2/Nw$ is the spin-relaxation constant calculated by Abragam and Pound (18). The frequency $\omega_{Q,f}$ is proportional to V^f_{ZZ}, the square root of the mean square value of the fluctuating EFG, and w is the jump rate between N stochastic states. Instead, V_{zz} (or ω_Q) and η signify the static contribution of the quadrupole interaction that results from the ensemble average of the EFG taken over N stochastic states. For slow perturbation, the relaxation parameter is proportional to the fluctuation rate w: $\lambda_2 = (N-1)w$ (19).

RESULTS

The spin precession curves for $I = 5/2$ and $Q = 2.8$b ^{181}Ta excited state vs delay time t at selected temperatures are shown in Fig. 1 (20). Changes in the perturbation factor are observed with increasing temperature. We will describe what follows in terms of two sites. The regular site ($f_1 > 90\%$) is the one where ^{181}Ta occupies the positions of Hf atoms in $SrHfO_3$ and it characterized by well defined hyperfine parameters. The second site ($f_2 < 10\%$) corresponds to probes in HfO_2 and indicates the presence of a small amount of this oxide without reacting.

In Fig. 2, the hyperfine parameters ω_Q, η, δ, and λ_2 resulting from fitting Eq. [2] to the PAC spectra measured as a function of temperature from RT to 1173 K are shown. At RT the regular site is characterized by the static hyperfine parameters $\omega_Q = 19.8_3$ Mrad/s, $\eta = 0.47_2$, and $\delta = 0.24_2$. From RT and up to 573 K the damping coefficient treated as a free parameter in the fitting procedure gave

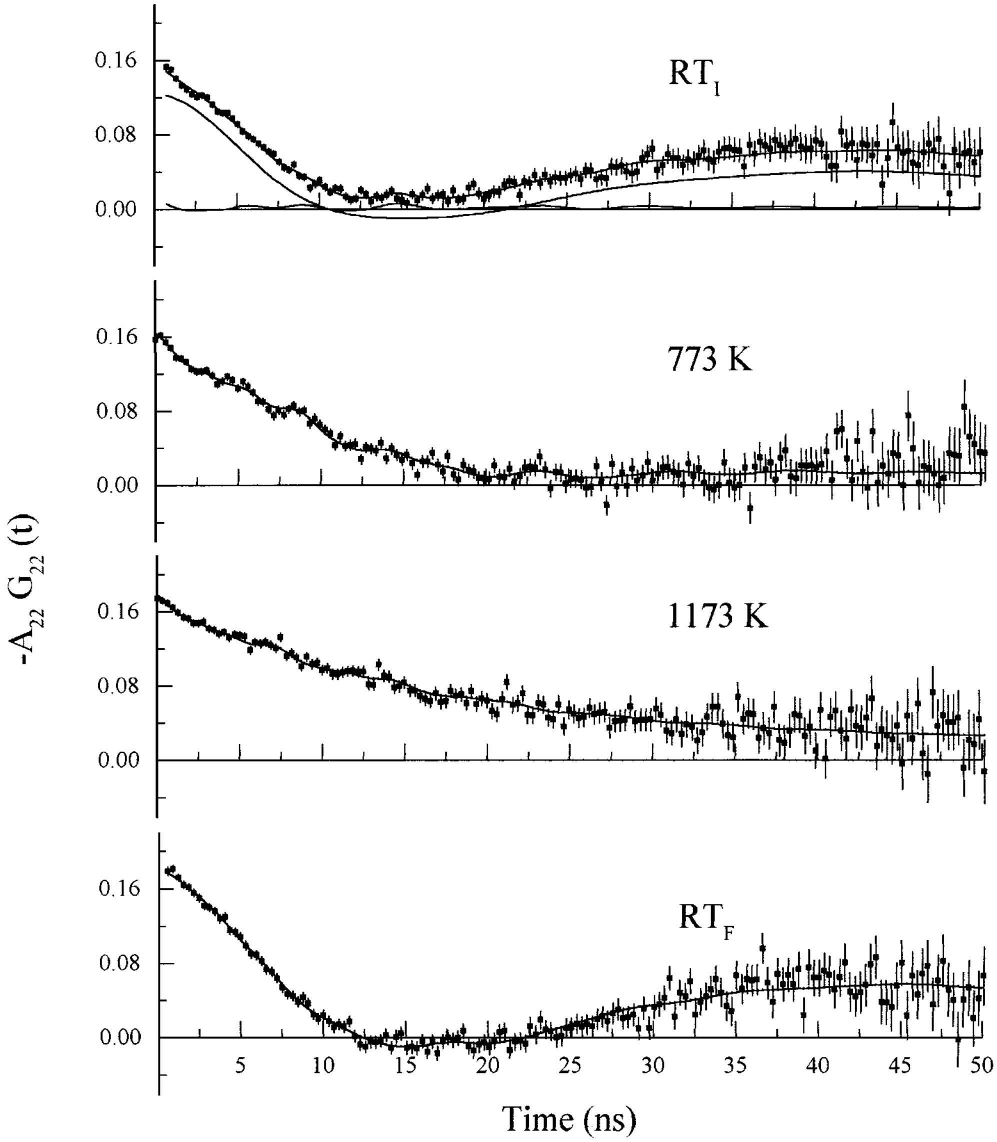

FIG. 1. Spin precession curves for ^{181}Ta probe in SrHfO$_3$ measured at the indicated temperatures. The solid lines represents the least-squared fits to the data. At RTI contributions of two quadrupole interactions fitted to the data are split up. For every spectrum $|c_0| \leq 0.02_1$.

$\lambda_2 \approx 0$ MHz, this small value being an artifact produced by the fit. For this reason we decided to fit it at zero in that temperature range, and the form of the perturbation factor corresponds to that produced by a static, asymmetric, and distributed electric quadrupole interaction. The thermal dependence of hyperfine parameters show that ω_Q decreases, η undergoes almost constant, and δ increase with temperature.

The temperature dependence of ω_Q, η, and δ has a discontinuity at $573 < T < 673$ K. For $673 < T < 873$ K the hyperfine parameters have behavior different from that of those measured at lower temperatures and a new feature appears: an attenuation parameter λ_2 that increases with temperature.

The quadrupole frequency seems to have a different slope, δ diminished down to $\sim$1% (but with large errors $\sim$100%), and keeps constant. Instead, it was not possible to determine the value of η because the value fitted was consistent with the initial value inserted. So we fix $\eta = 1$ for this temperature range. The other parameters and χ^2 were nearly unaffected by the adopted η value.

Above 873 K and up to 1173 K, the fit of time spectra was consistent with the initial values of ω_Q and η, and the resulting quadrupole parameters show extremely large errors. In fact, frequencies lower than $\sim$3 Mrad/s cannot be resolved by the spectrometer. Thus, they were fixed to zero and a nuclear spin relaxation process could be fitted with a relaxation parameter $\lambda_2 = 68_3$ MHz at 973 K.

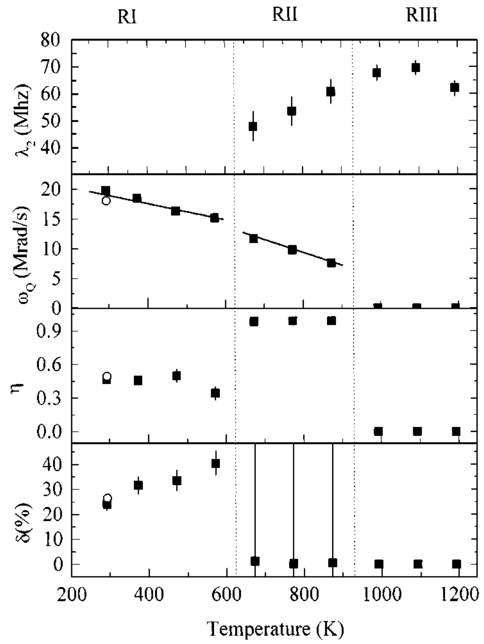

FIG. 2. Temperature dependence of the hyperfine parameters corresponding to ^{181}Ta probes in B sites of strontium hafnate is plotted. To guide the eye, the dotted line separates the different temperature dependence of the quadrupole parameters that correspond to the different structures determined by X-ray and neutron diffraction techniques, respectively. In the same way the thin lines showed in $\omega_Q(T)$ are to guide the eye.

For $T > 650$ K, the attempts to fit a static and distributed quadrupole interaction ($\lambda_2 = 0$) to the spin precession spectra yield hyperfine parameters with large errors in ω_Q and η with $\delta \gg 100\%$, matching these results with previous observations in other AMO_3 compounds (10).

The fitted hyperfine parameters corresponding to probes at the second site coincide with those already reported for ^{181}Ta probes in HfO_2 (21).

DISCUSSION

Low values of ω_Q (or V_{ZZ}) characterize the regular site and this is in agreement with the crystallographic data that show small differences (< 0.013 Å) between the lattice constants of the equivalent pseudocubic structure ($a' = 2^{-1/2}a, b' = 2^{-1/2}b, c' = 2^{-1}c$) corresponding to the true noncubic (a, b, c) lattice (5, 6).

From RT up to 573 K the quadrupole frequency decreases linearly with temperature from 19.8_3 to 15.1_6 Mrad/s, respectively. The asymmetry parameter is $\eta = 0.47_2$ at RT and decreases down to $\eta = 0.34_5$ at 573 K. High η values were measured by PAC in AMO_3 in structures with tilted oxygen octahedra. In these compounds high δ values are found and it is also common to observe that δ increases with temperature. The origin of this disorder was associated with random distribution of oxygen vacancies polarized by the impure state introduced by the probe.

From 673 K up to 973 K the structure is also orthorhombic. In this phase, ω_Q also decreases linearly with temperature but with different slope, η is undetermined, $\delta \approx 0$ but with large errors, and a relaxation process contributes to the perturbation. The indeterminancy of η presumably results from two effects: a very low frequency at these temperatures ($\omega_Q = 11.7_4$ Mrad/s at 673 K) combined with a relative short time window determined by the ^{181}Ta probe. However, in ^{111}Cd-implanted $SrHfO_3$ experiments the asymmetry parameters fitted in the high-temperature phase (RII) are higher than those fitted at lower temperatures, and then η should increase, justifying the value $\eta = 1$ adopted in this work. In these compounds phase transitions are sometimes characterized by δ values increasing for $T < T_C$ and having large relative errors for $T > T_C$, as is observed in Fig. 2.

Above 973 K, good fits were obtained if V_{zz}, η, and δ were set to 0. If the phase transition detected by diffraction analysis would not exist the extrapolated value ω_Q should be ≈ 5 Mrad/s. The resolution of the PAC spectrometer establish a lower limit of $\omega_Q \approx 3$ Mrad/s. Thus, the quadrupole frequency above 973 K should be close to zero (i.e., lower than ≈ 3 Mrad/s), which corresponds to an equivalent pseudocubic structure with $1 - c/a \approx 10^{-3}$ and this phase is characterized only by a nuclear relaxation process, as seen by PAC.

It has been observed that the ratio of quadrupole frequencies $\omega_Q(^{181}\mathrm{Ta})/\omega_Q(^{111}\mathrm{Cd})$ measured at the same site of same oxide is close to the value $6.5_{1.2}$, as estimated from the scaling of the correspondent quadrupole moments and Sternheimer factors of both probes (13). Besides, if the EFG at probes is produced only by the ions in the lattice, this ratio should be temperature-independent. In Fig. 3 the values of $\omega_Q(^{181}\mathrm{Ta})/\omega_Q(^{111}\mathrm{Cd})$ as a function of the temperatures is shown: at RT the ratio is 6.0_3, close to the value predicted. However, as the temperature increases the ratio diminishes and this effect seems to be more pronounced above $\sim$650 K. The temperature dependence of the quadrupole frequency (or V_{zz}) corresponding to each probe is different, as is observed if the ratio $\omega_Q(^{181}\mathrm{Ta,RT})/\omega_Q(^{181}\mathrm{Ta}, 873\ \mathrm{K}) = 2.61_6$ is compared to the value $\omega_Q(^{111}\mathrm{Cd,RT})/\omega_Q(^{111}\mathrm{Cd}, 873\ \mathrm{K}) = 1.9_2$. This result would indicate that other sources such as electron covalence and local effects would contribute to the EFG due to the different impurity states introduced by Ta (one electron) and Cd (two holes).

What is the origin of the time-dependent effect observed for $T > 650$ K? One very important thing to take into account for applying Eq. [2] or another model is the previous knowledge available about the system of interest. In $SrHfO_3$ there is not a priori any reason to suppose the presence of a fluctuating electric field gradient.

It is very important to point out the relative high values of δ for $SrHfO_3$ measured at low temperatures. At RT the

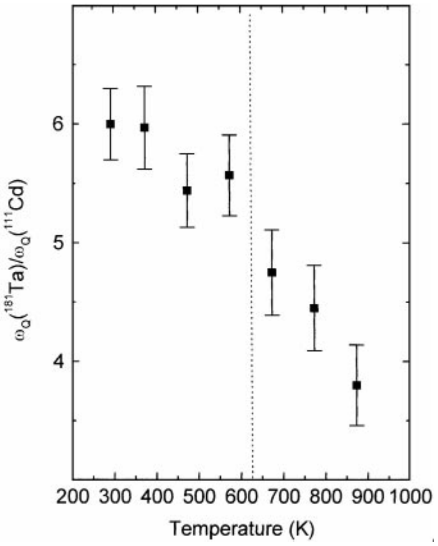

FIG. 3. The ratio $\omega_Q(^{181}\mathrm{Ta})/\omega_Q(^{111}\mathrm{Cd})$ is plotted vs temperature. The dotted line has the same meaning as in Fig. 2.

value is $\delta = 0.24_2$. As temperature increases, this parameter also increases (see Fig. 2). Similar behavior has been reported in the literature, as for example in Ref. (22), where PbTiO$_3$ is studied by PAC using Ta^{5+} probes. Most of the line-broadening effects were attributed to Ti ion jumps between sites that correspond to minima on a potential energy surface. For the case of a BaTiO$_3$–BaHfO$_3$ system (23), the large value of δ (also associated to dynamic effects) was explained in terms of the eight-site model's picture. On the other hand, in CdTiO$_3$ (22) and CaHfO$_3$ (9) samples the line-broadening is small (less than 5%), being almost constant or diminishing with the temperature. In these cases, δ describes lattice imperfections. Furthermore, there are no phase transitions in these compounds for all measured temperatures.

Thus, two effects would produce the relative line-broadening: one associated with static lattice imperfections (probably less than 5%) and the other coming from the contribution of a fluctuating EFG with temperature-dependent rates. At RT this process at a Ta probe in SrHfO$_3$ is *very slow*. As temperature increases, the measured line-broadening increases. This fact could be explained in the following way: as the temperature rises, the rate quickens and consequently allows the number of possible values of V_{zz} produced at probes to increase. The ensemble average of the interaction originates an asymmetric and disordered EFG.

Above 573 and below 973 K, in the *slow* jump rate region, w has to be several orders of magnitude faster than those jump rates typical for temperatures below 573 K. As a consequence a temperature-dependent spin-relaxation parameter appears, the line-broadening parameter decreases to zero, and the ensemble average of the quadrupole interaction results in an axially asymmetric EFG.

In the slow fluctuation rate regime, the relaxation caused by slow anisotropic fluctuation should be proportional to the jump rate. If the temperature dependence of the average jump rate w is given by the Arrhenius relation $w(T) = w_0 \exp(-E_a/kT)$, where E_a is the activation energy for over-barrier jumps, then $\ln \lambda_2 \propto (-E_a/kT)$. The fit of this expression to the data gave an activation energy $E_a = 80_6$ meV (see Fig. 4). This activation energy is too low to describe any ionic hopping process and probably would correspond to the excitation of electron impurity states.

At ^{111}Cd in SrHfO$_3$ samples similar time-dependent effects were observed but at lower temperatures. In fact the slow and fast regime occurs from ~600 to ~850 K (13). The model used to fit the hyperfine parameters predicts that the activation energies of both regimes should be the same (16, 17). The fitted values for the slow and fast regimes are 155_{30} and 177_{41} meV, respectively. These relaxation processes would correspond to the excitation of hole impurity states.

Above 973 K in ^{181}Ta at SrHfO$_3$ measurements, due to the fact that weak quadrupole interactions with $\omega_Q \leq 3$ Mrad/s cannot be resolved, only a time-dependent perturbation seems to act on probes, which corresponds to a fast relaxation hopping process. This time-dependent field was previously observed in other AMO$_3$ materials. For SrHfO$_3$, the value of this parameter is $\lambda_2 = 68_2$ MHz at 973 K, which is comparable to the value $\lambda_2 = 44_2$ MHz measured in BaHfO$_3$ in the same regime (10).

The temperature dependence of hyperfine parameters show discontinuities in all hyperfine parameters at the *Pnma*↔*Cmcm* phase transition: In RII the relaxation is evident and the EFG (ω_Q, η, and δ) jumps. Instead, the signals of the *Cmcm*↔*I*4/*mcm* phase transition are not as clear and seem to be continuous in the relaxation parameter. The continuity in the other quadrupole parameters was not as evident due to instrumental resolution that was

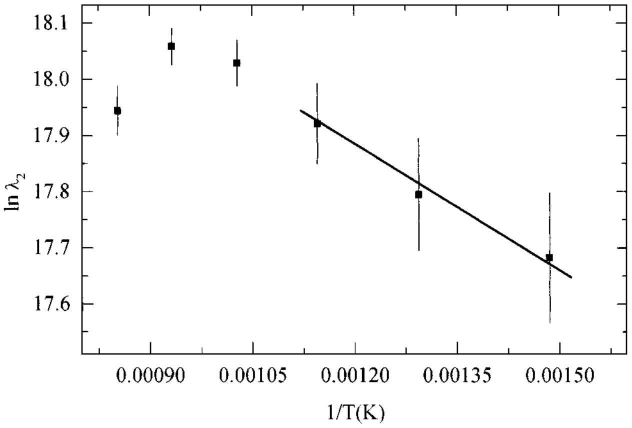

FIG. 4. The $\ln \lambda_2$ vs $1/T$ is shown. The straight line represents the least-square fit result.

not capable of determining the values of EFG tending to zero.

CONCLUSIONS

This PAC analysis of the quadrupole perturbations at probes in regular sites of $SrHfO_3$ from RT to 1173 K, allowed the determination of three time windows that occur at the same temperatures corresponding to three different crystalline structures that were determined by diffraction techniques. From room temperature to $\approx$600 K the very slow fluctuation results in a static, asymmetric, and disordered EFG. The line width would be produced by trapped electron states at randomly localized sites. From $\approx$600 to $\approx$950 K, it seems that the crystalline structure modifies the trapped electron impurity states, allowing a slow jump rate that increases with the temperature. The activation energy of this process is 80_6 meV. Above $\approx$950 K the same mechanism produce fast jumps and would originate an almost pure relaxation process. The observed temperature dependence of the $\omega_Q(^{181}\mathrm{Ta})/\omega_Q(^{111}\mathrm{Cd})$ ratio would indicate the effects of different electron covalence and local distortions produced by probes. Discontinuities in all hyperfine parameters at the *Pnma*↔*Cmcm* phase transition are observed. Instead the continuity of quadrupole parameters in the *Cmcm*↔*I*4/*mcm* phase transition is not as evident.

ACKNOWLEDGMENTS

UNLP, CONICET, and CICPBA of Argentina partially supported this work.

REFERENCES

1. A. Hoffman, *Z. Phys. Chem.* **28,** 74 (1935).
2. S. Naray-Szabó, *Muegy. Kozl.* **1,** 30 (1947).
3. V. P. Red'ko, A. V. Shevchenko, and L. M. Lopato, *Izv. Akad. Nauk SSSR, Neorg. Mater.* **19,** 2059 (1983).
4. F. Jona and G. Shirane, "Ferroelectric Crystals," International Series of Monographs on Solid State Physics, Chap. 5. Pergamon, Oxford, 1962.
5. J. A. Guevara, S. L. Cuffini, Y. P. Mascarenhas, R. E. Carbonio, J. A. Alonso, M. T. Fernández, P. de la Presa, A. Ayala, and A. López-García, *Mater. Sci. Forum* **278–281,** 720 (1998); S. L. Cuffini, J. A. Guevara, Y. P. Mascarenhas, P. de la Presa, A. Ayala, and A. López-García, Cerâmica **43,** 91 (1997).
6. B. J. Kennedy, C. J. Howard, and B. C. Chakoumakos, *Phys. Rev. B* **60,** 2972 (1999).
7. D. J. Singh, *Ferroelectrics* **153,** 183 (1994).
8. G. Fabricius, E. L. Peltzer y Blanca, C. O. Rodríguez, A. P. Ayala, P. de la Presa, and A. López-García, *Phys. Rev. B* **55,** 164 (1997).
9. P. de la Presa and A. López-García, *Radiat. Eff. Defects Solids* **140,** 141 (1997).
10. A. López-García, P. de la Presa, and A. M. Rodríguez, *Phys. Rev. B* **44,** 9768 (1991); A. López-García, P. de la Presa, A. M. Rodríguez, H. Saitovitch, and P. R. J. Silva, *Phys. Rev. B* **47,** 48 (1994).
11. K. C. Sebastian, D. R. S. Somayajulu, S. N. A. Jaffrey, S. S. Sharma, and J. Varma, *Hyp. Int.* **99,** 347 (1996).
12. P. de la Presa, R. E. Alonso, A. Ayala, S. Habenicht, V. V. Krishnamurthy, K. P. Lieb, A. López-García, M. Neubauer, and M. Uhrmacher, *J. Phys. Chem. Solids* **60,** 749 (1999).
13. P. da R. Andrade, M. Forker, J. D. Rogers and J. V. Kunzler, *Phys. Rev. B* **6,** 2560 (1972).
14. M. Blume, *Phys. Rev.* **174,** 351 (1968).
15. H. Winkler and E. Gerdau, *Z. Phys.* **262,** 363 (1973).
16. A. Baudry and P. Boyer, *Hyp. Int.* **35,** 803 (1987).
17. M. Forker, W. Herz, and D. Simon, *Nucl. Instrum. Methods Phys. Res. Sect. A* **337,** 534 (1994).
18. A. Abragam and R. V. Pound, *Phys. Rev.* **92,** 943 (1953).
19. A. G. Marshall and C. F. Meares, *J. Chem. Phys.* **56,** 1226 (1972).
20. R. B. Firestone, *Nucl. Data Sheet* **43,** 289 (1984).
21. A. Ayala, R. Alonso, and A. López-García, *Phys. Rev.* **50,** 3547 (1994).
22. G. L. Catchen, S. J. Wukitch, D. M. Spaar, and M. Blaskiewics, *Phys. Rev. B* **42,** 1885 (1990).
23. A. Ayala and A. López-García, *Hyperfine Interact. C* **1,** 364 (1996).